Supporting Information

Dynamic Neighbouring Participation of Nitrogen Lone Pairs on the Chromogenic Behaviour of *trans*-Bis(salicylaldiminato)Pt(II) Coordination Platforms

Takumi Hashimoto, Kanako Fukumoto, Ngoc Ha-Thu Le, Tatsuya Matsuoka, Soichiro Kawamorita, Naruyoshi Komiya, and Takeshi Naota

Department of Chemistry, Graduate School of Engineering Science, Osaka University
Machikaneyama, Toyonaka, Osaka 560-8531, Japan

Contents

(a)

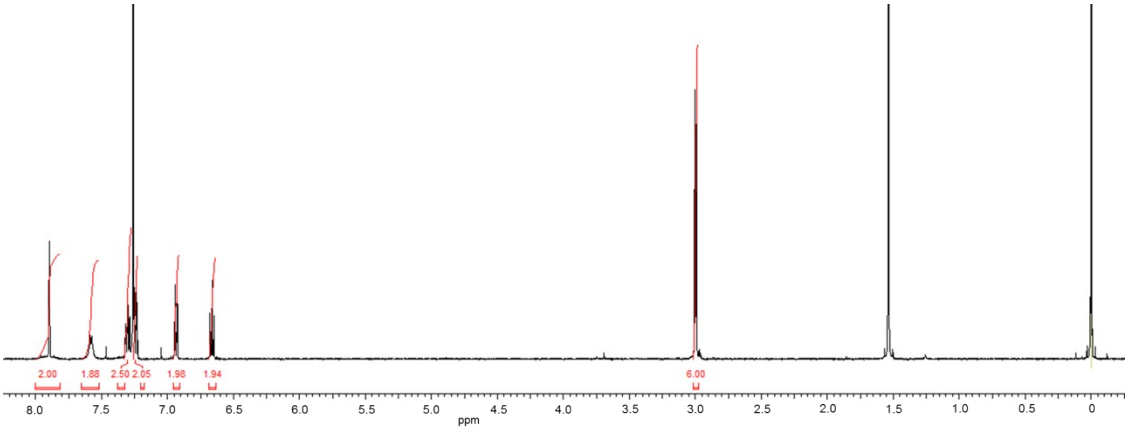

(b)

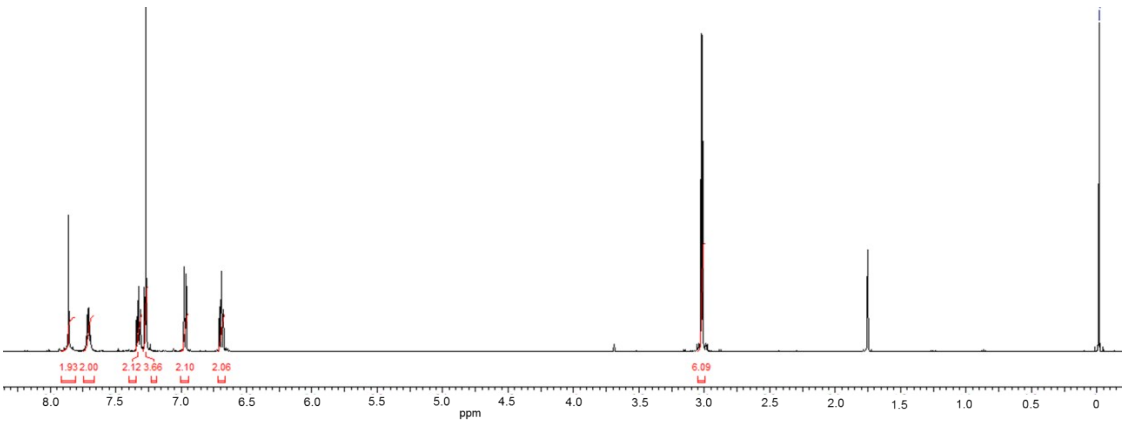

Fig. S1 ^{1}H NMR (500 MHz) spectra of **1a** at (a) 298 K and (b) 243 K in $CDCl_3$.

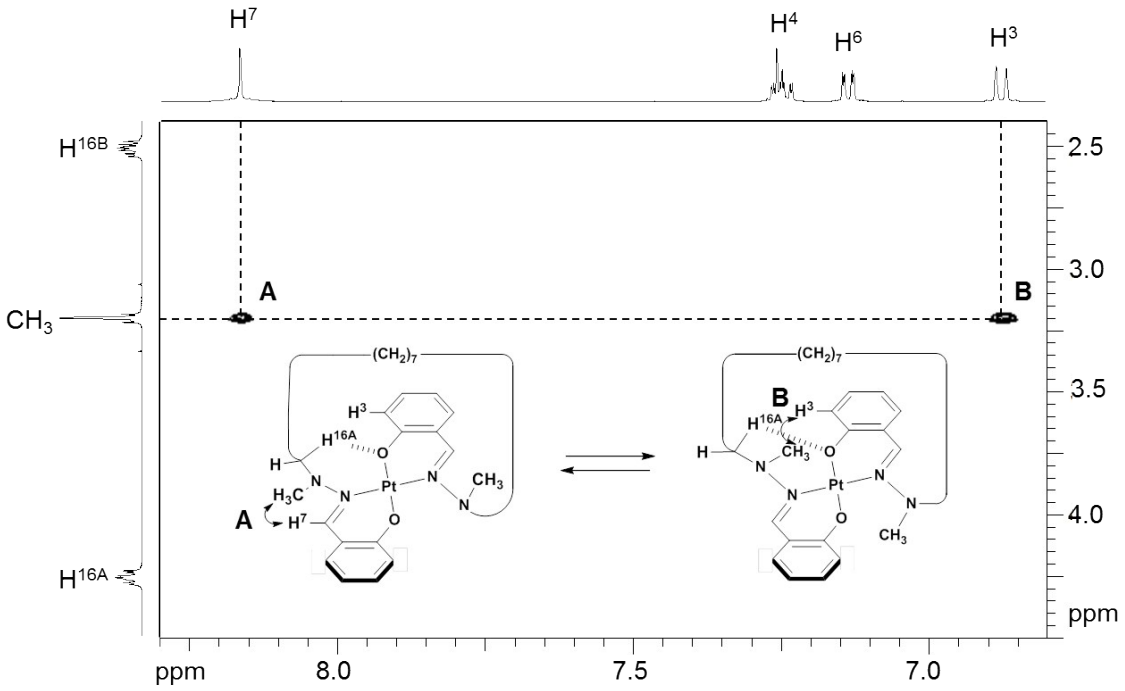

Fig. S2 NOESY spectrum (500 MHz) of **3** in $CDCl_3$ (298 K, mixing time = 0.4 s, number of t_1 increments = 1024, number of t_2 increments = 512, number of scans = 68).

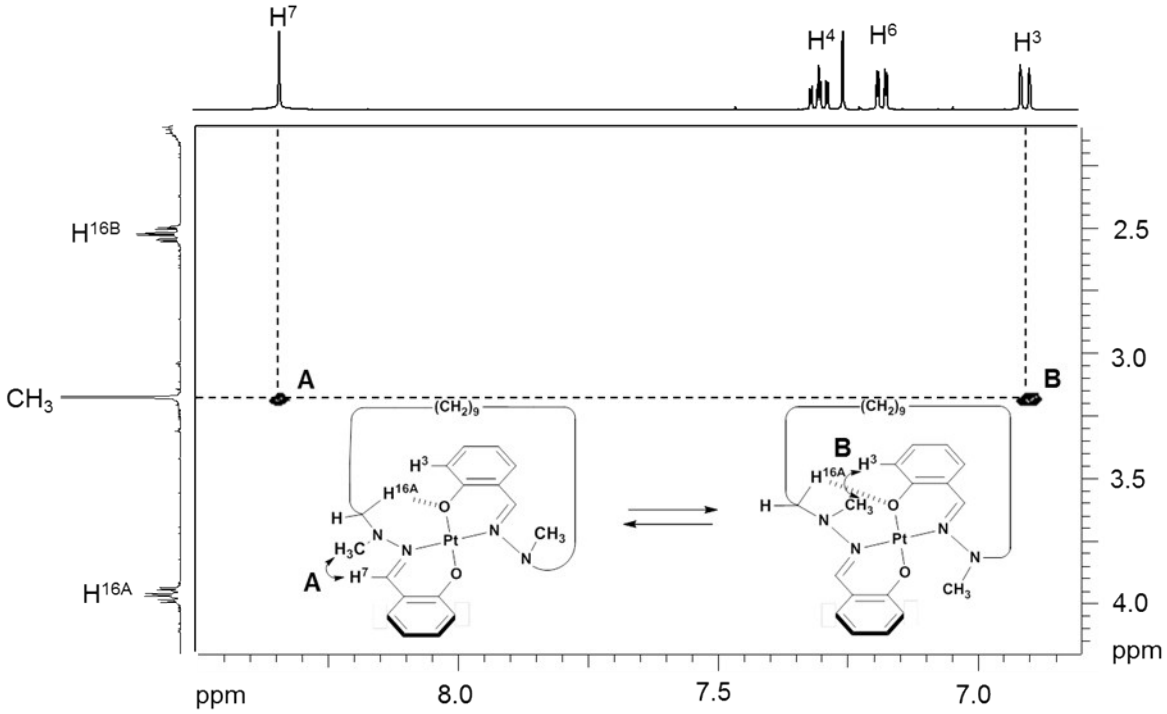

Fig. S3 NOESY spectrum (500 MHz) of **4** in $CDCl_3$ (298 K, mixing time = 0.4 s, number of t_1 increments = 1024, number of t_2 increments = 512, number of scans = 68).

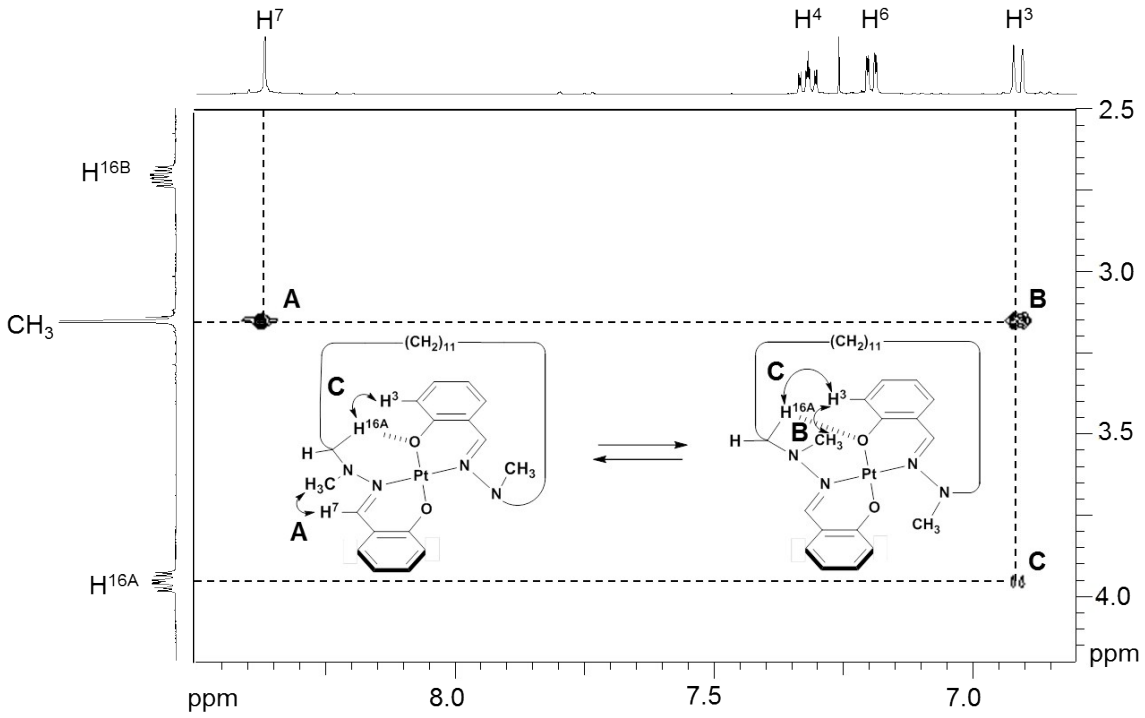

Fig. S4 NOESY spectrum (500 MHz) of **5** in $CDCl_3$ (298 K, mixing time = 0.4 s, number of t_1 increments = 1024, number of t_2 increments = 512, number of scans = 68).

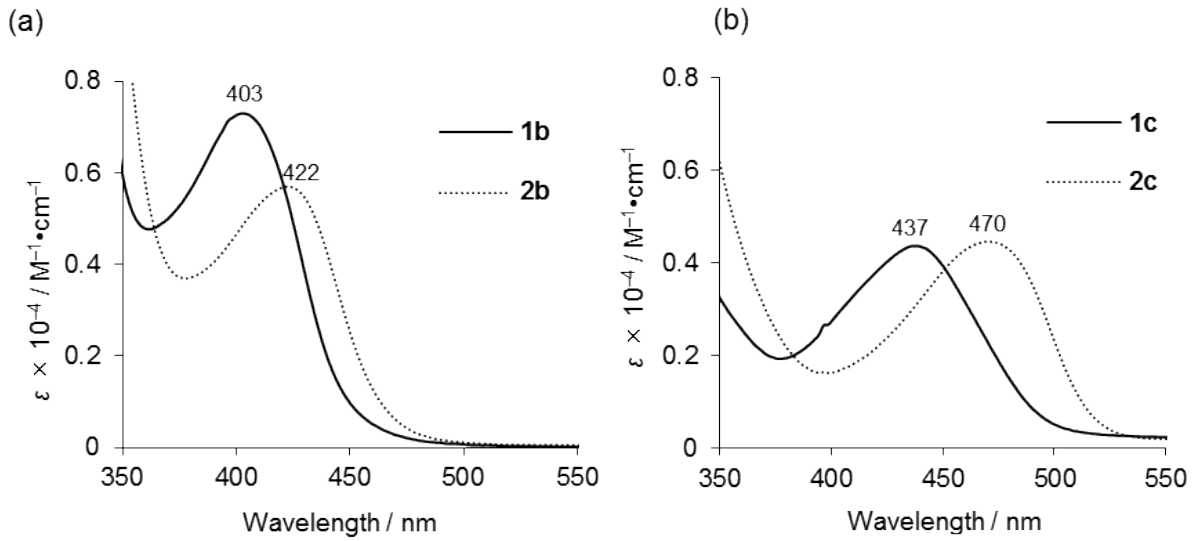

Fig. S5 UV–vis spectra of 2.0×10^{-4} M solutions of (a) **1b**, (b) **1c**, (a) **2b**, and (b) **2c** in CH_3CN at 298 K.

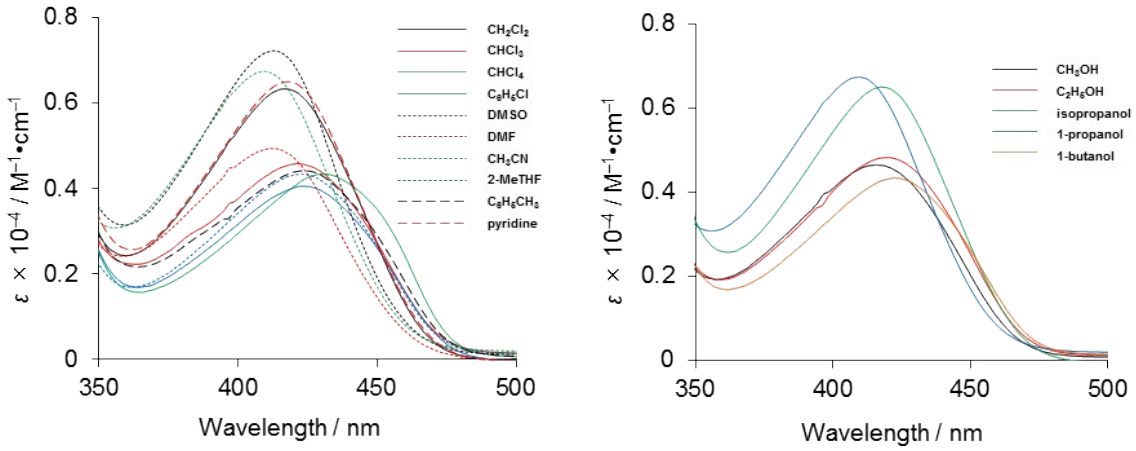

Fig. S6 UV–vis spectra of 2.0×10^{-4} M solutions of **1a** in various solvents at 298 K.

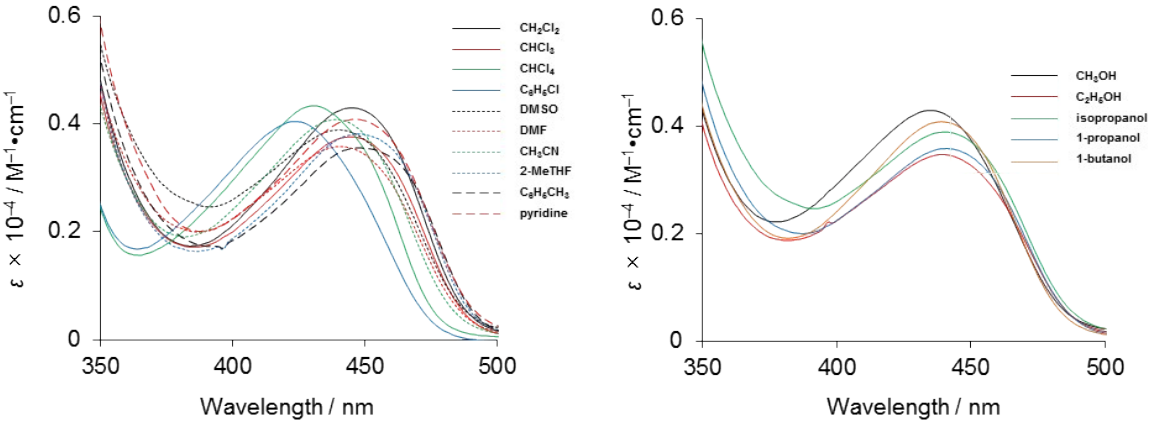

Fig. S7 UV–vis spectra of 2.0×10^{-4} M solutions of **2a** in various solvents at 298 K.

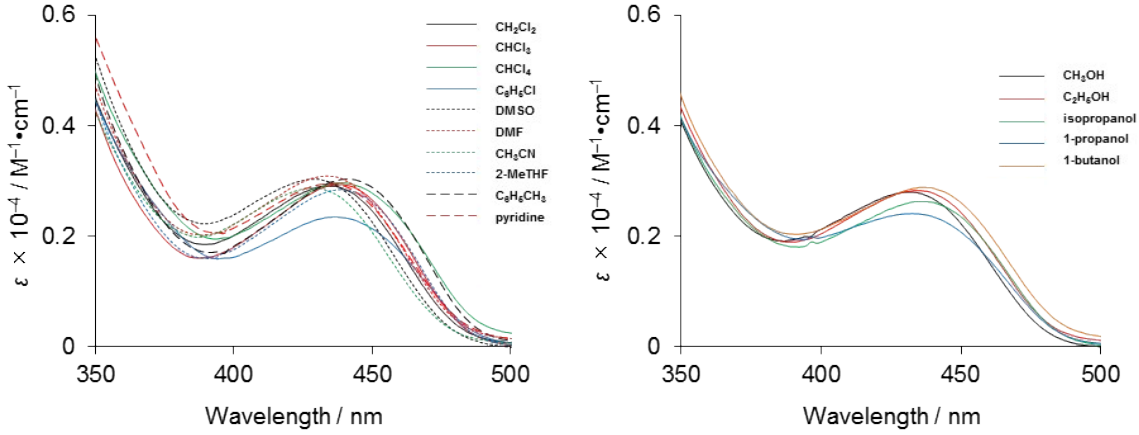

Fig. S8 UV–vis spectra of 2.0×10^{-4} M solutions of **3** in various solvents at 298 K.

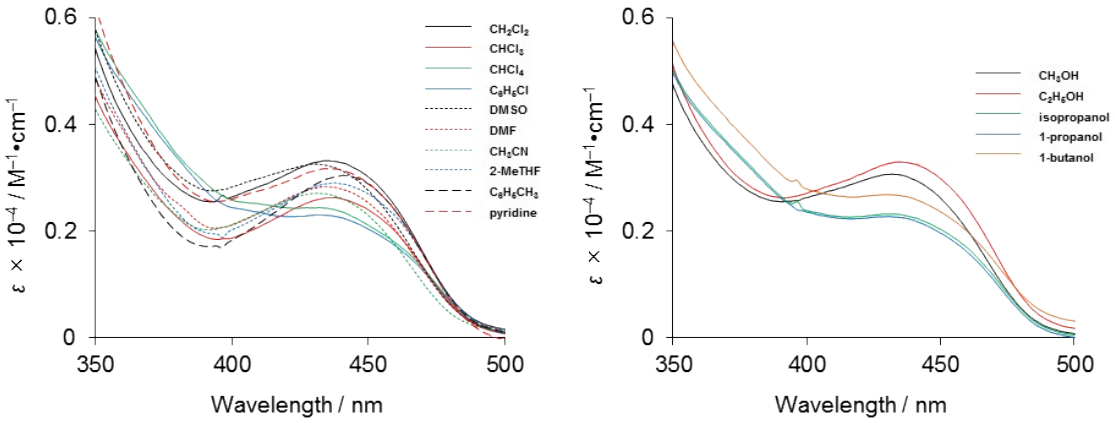

Fig. S9 UV–vis spectra of 2.0×10^{-4} M solutions of **4** in various solvents at 298 K.

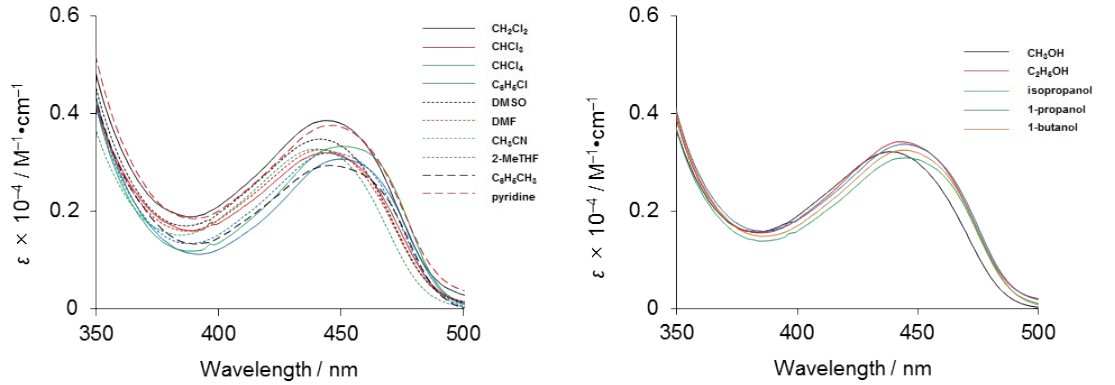

Fig. S10 UV–vis spectra of 2.0×10^{-4} M solutions of **5** in various solvents at 298 K.

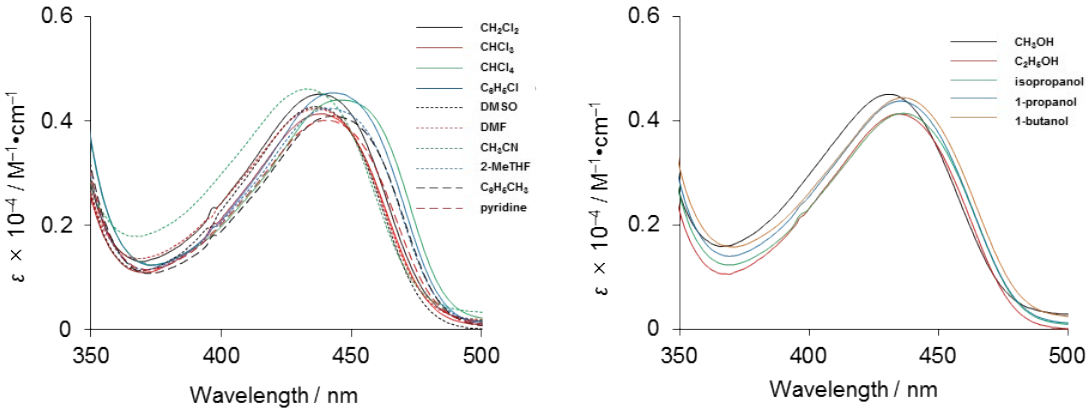

Fig. S11 UV–vis spectra of 2.0×10^{-4} M solutions of **6** in various solvents at 298 K.

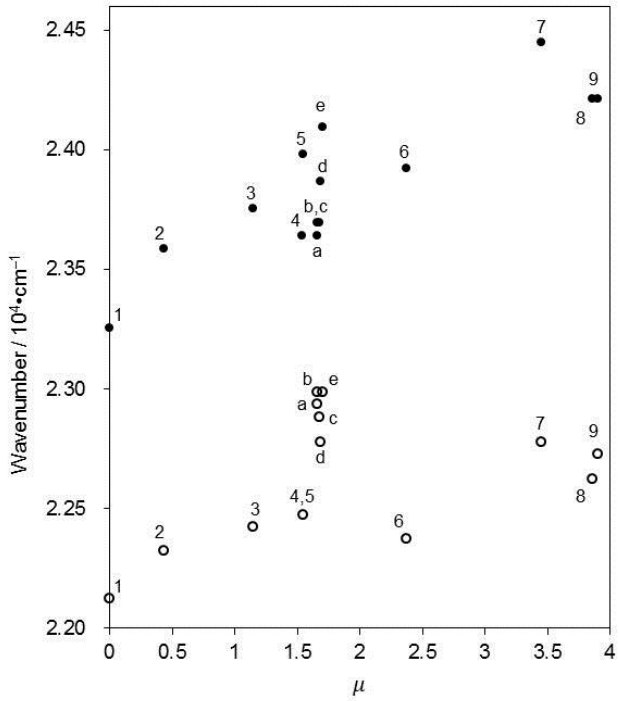

Fig. S12 Plot of ν_{max} (MLCT/ILCT) for **1a** and **2a** at 298 K against dipole moment μ values. ●: **1a**; ○: **2a.** Solvents: 1, CCl_4; 2, toluene; 3, $CHCl_3$; 4, chlorobenzene; 5, CH_2Cl_2; 6, pyridine; 7, CH_3CN; 8, DMF; 9, DMSO; a, isopropanol; b, 1-butanol; c, 1-propanol; d, ethanol; e, methanol.

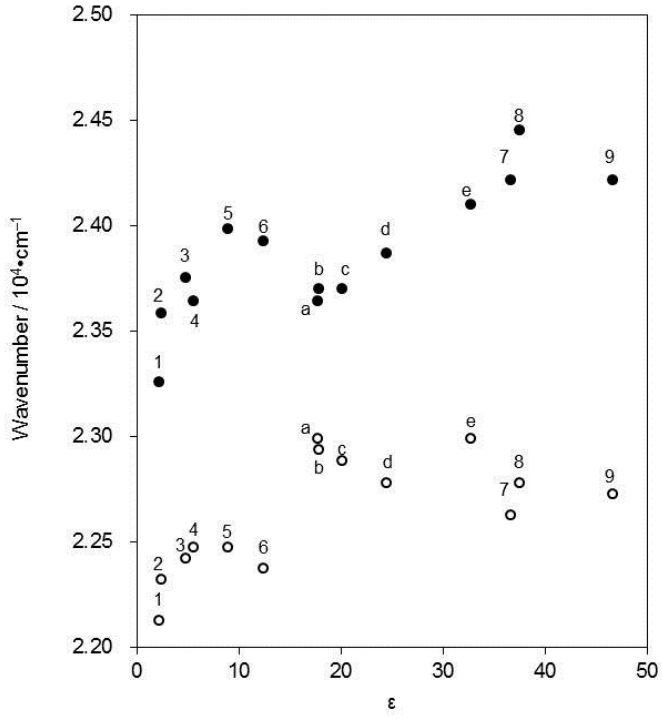

Fig. S13 Plot of ν_{max} (MLCT/ILCT) for **1a** and **2a** at 298 K against dielectric constant ε values. ●: **1a**; ○: **2a.** Solvents: 1, CCl_4; 2, toluene; 3, $CHCl_3$; 4, chlorobenzene; 5, CH_2Cl_2; 6, pyridine; 7, DMF; 8, CH_3CN; 9, DMSO; a, 1-butanol; b, isopropanol; c, 1-propanol; d, ethanol; e, methanol.

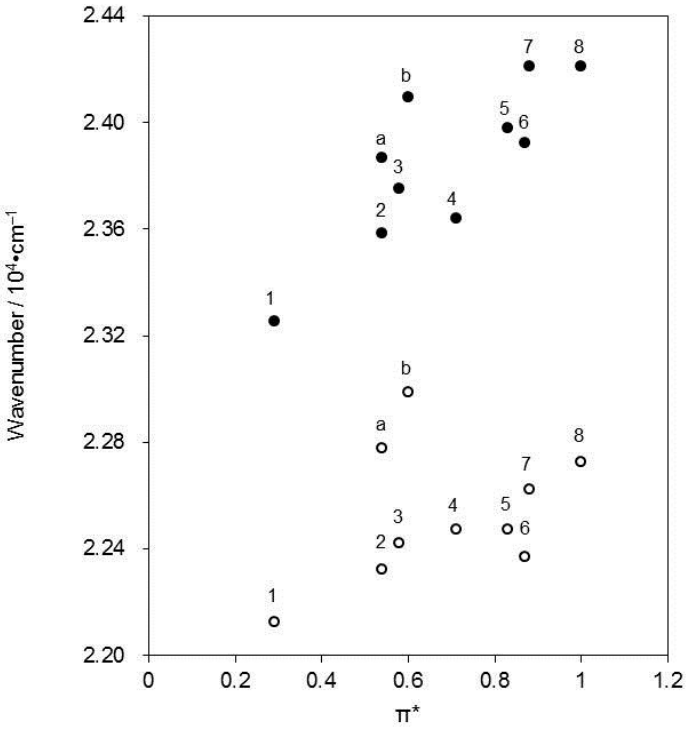

Fig. S14 Plot of ν_{max} (MLCT/ILCT) for **1a** and **2a** at 298 K against Kamlet and Taft's solvent polarity scale π* values. ●: **1a**; ○: **2a.** Solvents: 1, CCl_4; 2, toluene; 3, $CHCl_3$; 4, chlorobenzene; 5, CH_2Cl_2; 6, pyridine; 7, DMF; 8, DMSO; a, ethanol; b, methanol.

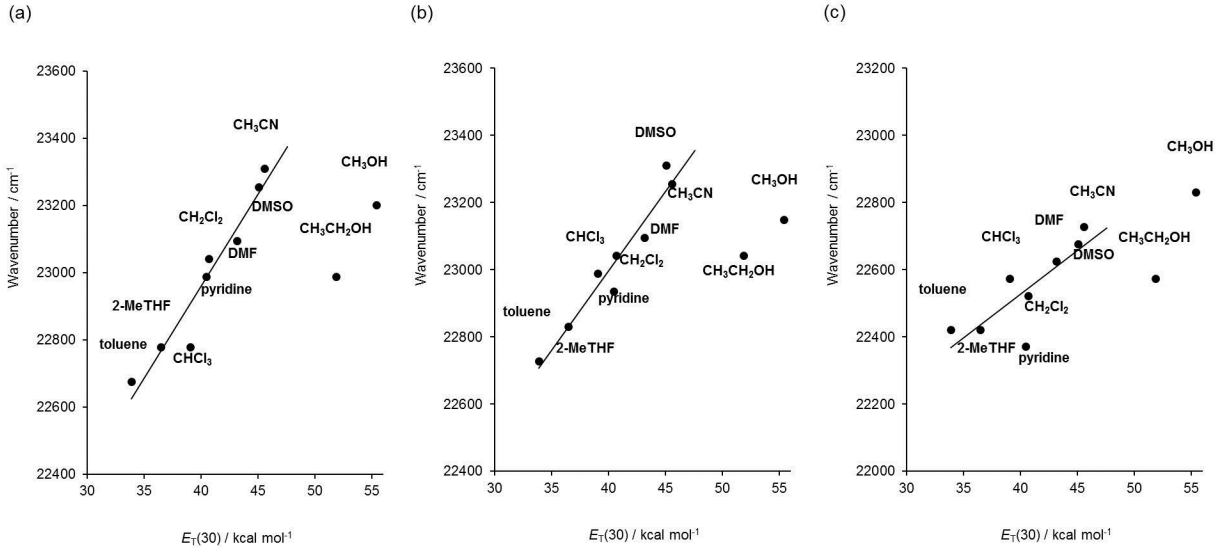

Fig. S15 Plots of ν_{max} (MLCT/ILCT) of (a) **3** , (b) **4** , and (c) **5** at 298 K against $E_T(30)$ solvent values.

Table S1 Calculated singlet transitions and major electronic contributions of **1a**, **2a**, **3**, **4**, **5**, and **6**[a]

Complex	State	Excitation energy / eV (nm)	Major configuration
1a	S1	2.85 (434)	HOMO → LUMO (49.1%)
	S2	3.16 (393)	HOMO → LUMO+1 (48.4%)
	S3	3.36 (369)	HOMO → LUMO+2 (46.8%)
2a (conformer II)	S1	2.84 (436)	HOMO →LUMO (49.0%)
	S2	3.10 (400)	HOMO → LUMO+1 (48.3%)
	S3	3.20 (388)	HOMO → LUMO+2 (46.7%)
2a (conformer III)	S1	2.78 (446)	HOMO → LUMO (49.0%)
	S2	2.94 (422)	HOMO → LUMO+1 (42.2%)
	S3	3.33 (372)	HOMO → LUMO+2 (38.0%)
3	S1	2.83 (438)	HOMO → LUMO (45.7%)
	S2	3.09 (401)	HOMO → LUMO+1 (47.5%)
	S3	3.28 (378)	HOMO → LUMO+2 (42.7%)
4	S1	2.83 (439)	HOMO → LUMO (46.7%)
	S2	3.09 (401)	HOMO → LUMO+1 (48.1%)
	S3	3.21 (386)	HOMO → LUMO+2 (44.4%)
5	S1	2.83 (438)	HOMO → LUMO (47.8%)
	S2	3.10 (400)	HOMO → LUMO+1 (48.0%)
	S3	3.23 (384)	HOMO → LUMO+2 (45.4%)
6	S1	2.85 (436)	HOMO → LUMO (49.1%)
	S2	3.12 (398)	HOMO → LUMO+1 (47.5%)
	S3	3.30 (376)	HOMO → LUMO+2 (45.9%)

---

[a] Estimated from TD-DFT calculations (B3LYP/6-31G*, LanL2DZ) based on the optimized structures.

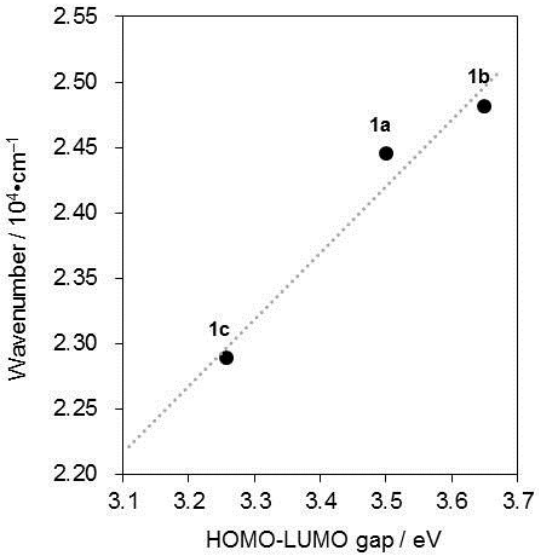

Fig. S16 Relationship between the HOMO–LUMO energy gap (eV) and wavenumber (cm^{-1}) at the absorption maxima around 350–500 nm for **1** at 298 K in CH_3CN. The energy gaps were estimated from DFT (B3LYP/6-31G*, LanL2DZ) calculations based on the optimized geometries.

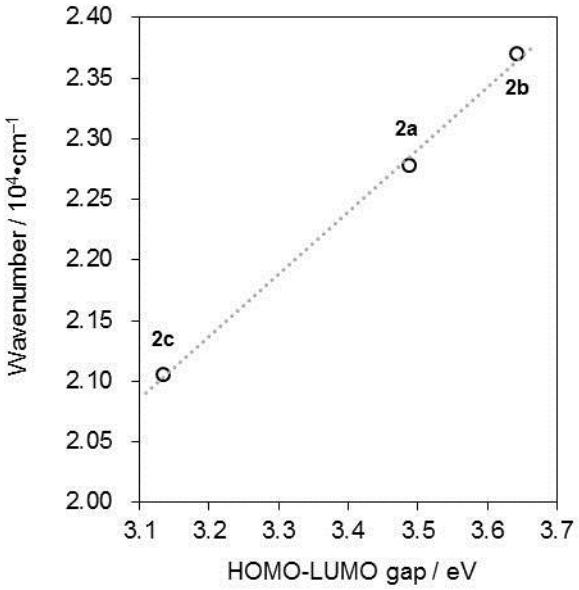

Fig. S17 Relationship between the HOMO–LUMO energy gap (eV) and wavenumber (cm^{-1}) at the absorption maxima around 400–500 nm for **2** at 298 K in CH_3CN. The energy gaps were estimated from DFT (B3LYP/6-31G*, LanL2DZ) calculations based on the optimized geometries.

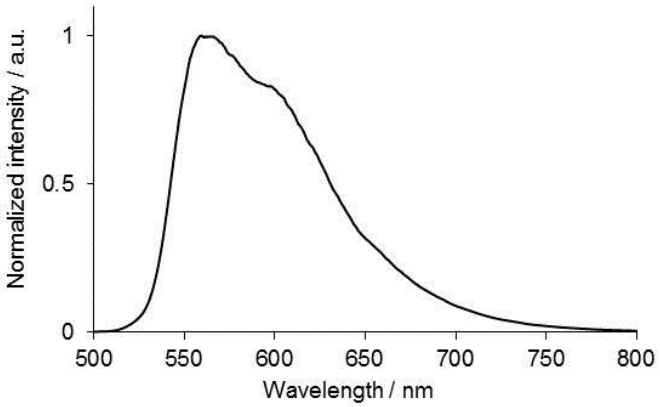

Fig. S18 Emission spectra of 2.0×10^{-4} M solution **6** in DMSO at 77 K ($\boldsymbol{\lambda}_{ex}$ = 450 nm).